Spectroscopy 22 (2008) 21–31
DOI 10.3233/SPE-2008-0340
IOS Press

Analysis of postmortem metabolic changes in rat kidney cortex using Fourier transform infrared spectroscopy

Ping Huang [a], Yong Ke [a], Qinyang Lu [a], Bo Xin [a], Shuanliang Fan [a], Guangde Yang [b] and Zhenyuan Wang [a,*]

[a] *Department of Forensic Medicine, School of Medicine, Xi'an Jiaotong University, Xi'an, P. R. China*
[b] *Institute of Chemical Analysis Research, Xi'an Jiaotong University, Xi'an, P. R. China*

Abstract. Estimation of the time since death (postmortem interval, PMI) is one of the most difficult problems in forensic investigations and many methods currently are utilized to estimate the PMI. The aim of this study was to investigate the changes of Fourier transform infrared (FT-IR) spectra of rat kidney cortex from time zero to 168 h postmortem at molecular level. The spectra of rat kidney cortex displayed the prominent changes with increasing postmortem interval. (1) Significant increase in the intensity of the C–H stretching bands at 2958, 2925, 2871, 2852 cm^{-1}, the =C–H stretching band at 3012 cm^{-1}, the $CO_2{}^-$ symmetric stretching band at 1396 cm^{-1} and the N–H bend, C–N stretching at 1541 cm^{-1}; (2) significant decrease in the intensity of the $PO_2{}^-$ stretching band at 1238, 1080 cm^{-1}; (3) the intensity of at 3303, 1652 and 1170 cm^{-1} remained relatively stable. The linear regression analysis of the various absorption intensity and area ratios against the PMI shows a close correlation, maximum for A_{1541}/A_{1396} ratio ($R^2 = 0.95$) and minimum for I_{1080}/I_{1396} ratio ($R^2 = 0.70$). Our results indicate that FT-IR spectroscopy may be a useful technique for estimating the short- and long-term PMI.

Keywords: Postmortem interval, kidney cortex, Fourier transform infrared spectroscopy, linear regression

1. Introduction

The postmortem interval (PMI) refers to the time since death, and estimation of PMI is extremely important in criminal, civil and forensic investigations. An accurate determination of the PMI can help reconstruct a crime scene, differentiate between homicide and suicide, and pinpoint a suspect, etc. Many methods have been attempted to accurately determine the PMI. These include examination of external physical characteristics of the body, chemical changes of body fluids, stomach contents and cadaveric temperatures [1–7].

Following clinical death, a number of complicated chemical reactions continue to occur within cells due to the remaining functional enzymes. which may presumably cause specific time-dependent changes in metabolism and sub-cellular structures that may be used to determine PMI. Indeed, many sophisticated methods have been used to find reliable markers for the estimation of PMI, including the analysis of potassium concentration in vitreous humor [8–11] and postmortem protein degradation within different tissues [12,13]. In addition, some researches have been focused on the degradation of nucleic acid

*Corresponding author: Zhenyuan Wang, School of Medicine, Xi'an Jiaotong University, Xi'an 710061, P. R. China. Tel.: +86 29 82655472; Fax: +86 29 82655472; E-mail: wzy218@mail.xjtu.edu.cn.

including DNA and RNA [14–16]. However, these methods require specialized laboratory analysis and sophisticated chemical procedures. It remains a challenge for forensic scholars to look for simpler and more efficient methods to determine PMI.

Fourier transform infrared (FT-IR) spectroscopy has become an increasingly powerful analytical tool in biochemistry, biophysics, biomedicine and molecular biology due to its high sensitivity in detecting the changes in the functional groups belonging to tissue components, such as proteins, lipids, nucleic acids and carbohydrates, etc. In recent years, the quantitative analysis using FT-IR spectroscopy has been used in many scientific fields, such as the environmental detection, the diagnosis of cancers and other disorders [17–24].

The FT-IR spectroscopy is a non-chemical procedure as opposed to other bio-molecular methods that may influence the chemical reaction within the postmortem tissues. In the present study, we investigated the postmortem changes on an experimental animal model. The rat kidney cortex was investigated at the molecular level by detecting the different functional groups using FT-IR spectroscopy. The kidney cortex tissue was selected due to be autolysis easily based on the histological observation. The enzymes in kidney cortex tend to be more active and putrefaction occurs early. The correlation between the different intensity and area ratios and the PMI was investigated using linear regression analyses based on FT-IR data, which to our knowledge, has not been reported previously.

2. Materials and methods

2.1. Animal specimens

Male Sprague–Dawley rats ($n = 10$, 240–260 g) provided by the Animal Center of Xi'an Jiaotong University were sacrificed by cervical dislocation and the cadavers were kept in a controlled environment chamber set at 20($\pm$2)°C. The kidney cortex were sub-sampled from the same rat at time zero, 12, 24, 48, 72, 96, 120, 144, 168 h (9 readings in each of ten rats; $n = 90$). The kidney cortex was selected because the kidney cortex tends to be autolysis easily and earlier than other tissues based on the histological observation. The tissues were placed into 2.5 ml cylindrical tubes and frozen immediately in liquid nitrogen. All of the animal experiments in the present study were performed in accordance with the principles for the Care and Use of Laboratory Animal Committee of Xi'an Jiaotong University.

2.2. Sample preparation

The tissues were freeze-dried *in vacuo* at -50°C 12 h for dehydration. About 2 mg of freeze-dried tissue was mixed with 200 mg of KBr, ground with an agate mortar and pestle for 5 min and then pressed into a pellet for 1 min using a force of 10 tons. The measured thickness of the pellets was 0.4 mm and the diameter was 12 mm.

2.3. FT-IR spectral measurement

The FT-IR spectra were recorded quantitatively at room temperature in the range 4000–400 cm^{-1} on a Shimadzu 8400S spectrometer. The spectrometer was kept on continuously to minimize warm-up instability and was purged continuously with dry air to eliminate interference by atmospheric water vapor. Interferograms were averaged for 100 scans at 4 cm^{-1} resolution. IR solution 1.10 software (Shimadzu corporation, Japan) was used for analysis of the FT-IR spectra and for recording the data from

the spectra (including the calculations of peak position, band intensity and area). Baseline correction was done for all the original spectra and I_x represents the infrared absorption intensity at wave-number x cm^{-1} and A_x represent the infrared absorption area at wave-number x cm^{-1}.

2.4. Statistical analysis

Statistical analysis was conducted by evaluating the mean values of ratio of band intensity and area per sample. The experimental replicates were averaged and the mean values ± SD was calculated for each time point. Linear regression analysis between band intensity and area ratios and PMI were performed. Linear regression analysis yielded the equations ($Y = Ax + B$) with a coefficient of determination (R^2). p values of less than 0.05 were regarded as being significant. All statistical analysis of the data was performed by using SPSS 11.5 software (SPSS Inc., USA).

3. Results and discussion

3.1. General FT-IR findings

The FT-IR original spectrum of rat kidney cortex were complex consisting of many bands arising from different functional groups belonging to lipids, carbohydrates, proteins, and nucleic acids. Moreover, the biological tissues have a lot of different kinds of components including prenchymal, mesenchymal, and blood. So FT-IR spectra of the kidney cortex are delivering sum spectra of these components. The 16 major absorption bands were elicited for analyzing the changes of chemical functions. To normalize the quantitative analysis of absorption bands, the intensity and area ratios of the different absorption bands were considered.

The detailed spectra analysis were performed in three distinct frequency ranges, namely between 3600–2800, 1700–1375, 1300–900 cm^{-1}. The enlarged original spectra at different time point from 0 to 168 h postmortem in the 3600–2800, 1700–1375, 1300–900 cm^{-1} were plotted together in Fig. 1. The 16 major bands were selected and assigned in Table 1. As demonstrated in Fig. 2, four full complete FT-IR spectra showed the changes of the 16 major bands at 0, 24, 72 and 168 h postmortem. The intensity or accurately the area of the absorption bands is directly related to the concentration of the molecules [19, 20,22,25]. Furthermore, the mean values (±SD) of band intensity and area ratios, derived from all of the ten cadavers, at each time point postmortem were shown in Figs 3–5. The linear regression correlations of the intensity and area ratios against PMI were plotted by the dotted lines in Figs 3–5. The linear regression equations of the different intensity and area ratios were demonstrated in Table 2. The peak position of 16 absorption bands remained relatively stable in their own stretching ranges from 0 h to 168 h postmortem.

3.2. The absorption band region at 3600–2800 cm^{-1}

As shown in Fig. 1(a), the region of 3600–2800 cm^{-1} presented 6 major absorption bands at 3303, 3012, 2958, 2925, 2871, 2852 cm^{-1}. The intensity of the band at 3303 cm^{-1} remained stable, which contains a strong absorption arising mainly from the N–H stretching (amide A) mode of protein with the contribution of the OH stretching modes in H_2O, polysaccharides [17,20]. As it can be seen from Fig. 1(a) and Fig. 2, there was a dramatic increase in this region whose spectrum is populated by absorptions stemming from the C–H stretching vibrations of olefinic =CH, –CH_2 and −CH_3 groups [18,19,23,25].

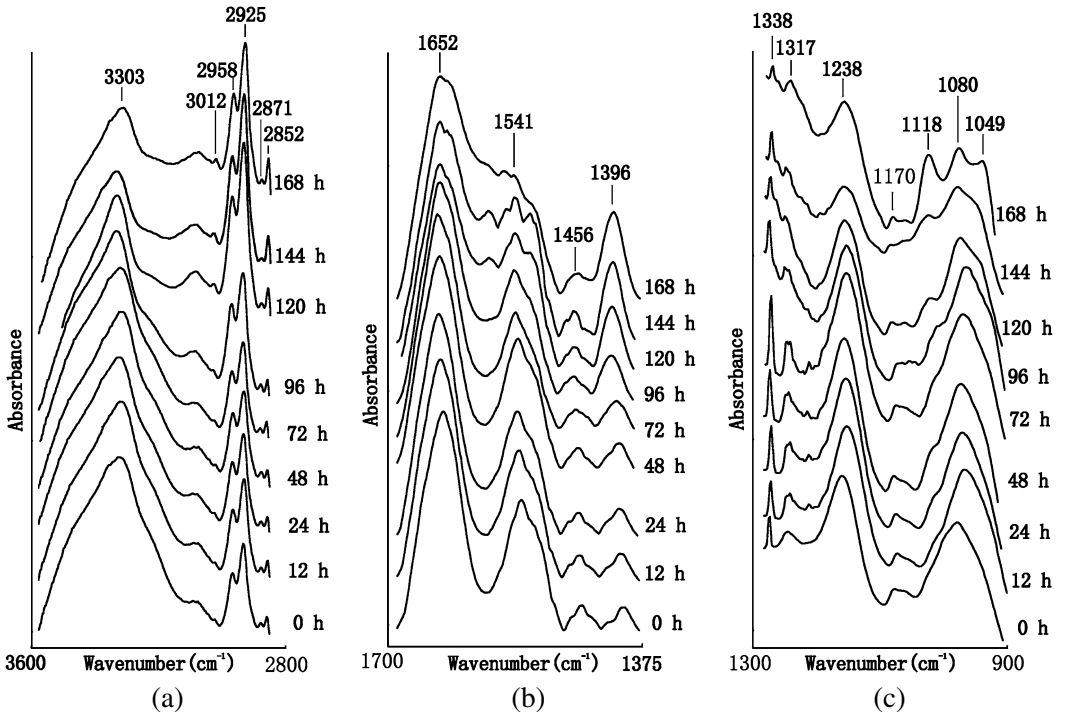

Fig. 1. Time-course of enlarged FT-IR original spectra from 0 to 168 h postmortem in rat kidney cortex at 20°C. (a) 3600–2800 cm^{-1} region; (b) 1700–1375 cm^{-1} region; (c) 1300–900 cm^{-1} region.

Table 1
Major absorption in the FTIR spectra of rat kidney cortex

Band numbers	Range (cm^{-1})	Present position (cm^{-1})	Assignments
1	3300–3500	3303	Maily N–H stretching (amide A)
2	3010–3014	3012	=C–H stretching
3	2956–2960	2958	CH_3 asymmetric stretching
4	2920–2925	2925	CH_2 asymmetric stretching
5	2870–2876	2871	CH_3 symmetric stretching
6	2850–2854	2852	CH_2 symmetric stretching
7	1600–1690	1652	Amide I (protein C=O stretching)
8	1480–1575	1541	Amide II (protein N–H bend, C–N stretching)
9	1452–1458	1454	CH_2 bending
10	1390–1400	1396	CO_2^- symmetric stretching
11	1330–1340	1338	CH_2 wagging stretching
12	1236–1240	1238	PO_2^- asymmetric stretching
13	1150–1190	1170	C–OH bending, CO–O–C asymmetric stretching
14	1118–1120	1118	Unconfirmed
15	1078–1083	1080	PO_2^- symmetric stretching
16	1029–1049	1049	C–O stretching

Band assignment (see [20–29]).

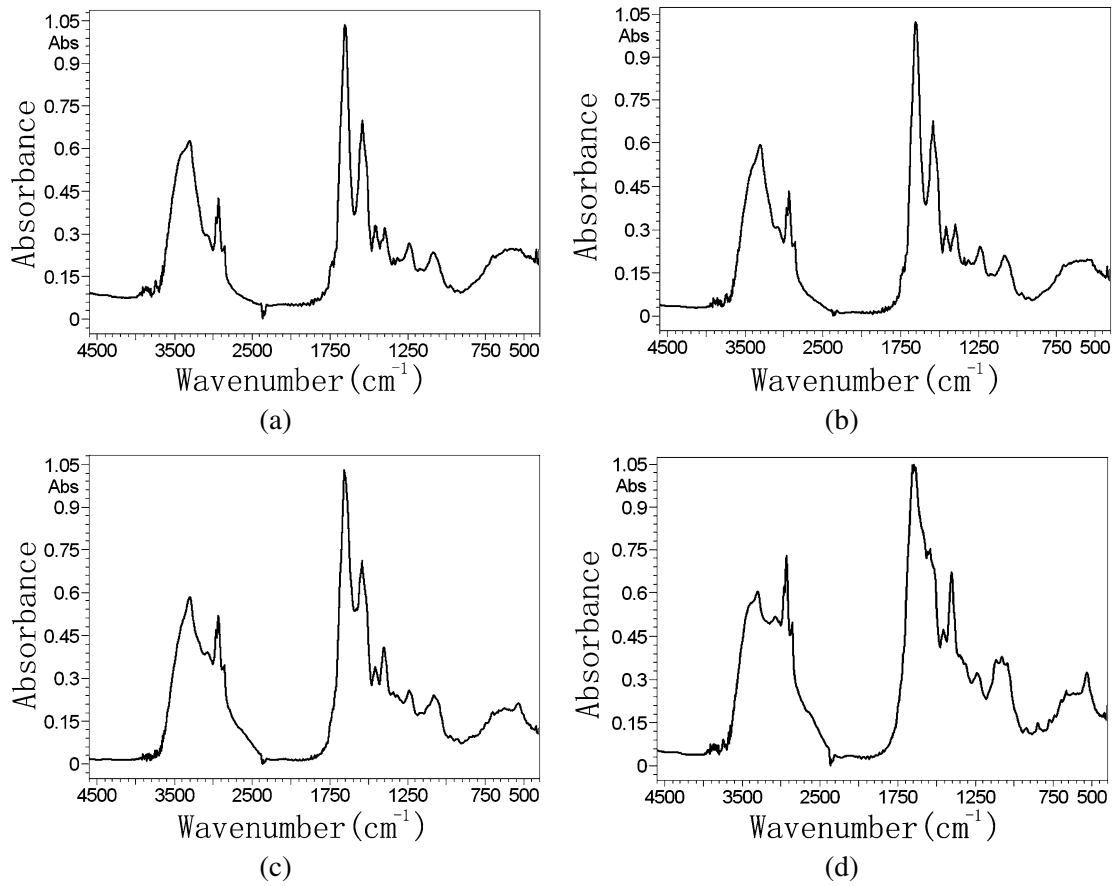

Fig. 2. Four complete FT-IR original spectra (a) 0 h, (b) 24 h, (c) 72 h and (d) 168 h postmortem.

As illustrated in Fig. 3(a)–(e), the I_{3012}/I_{3303}, I_{2958}/I_{3303}, I_{2925}/I_{3303}, I_{2871}/I_{3303}, I_{2858}/I_{3303} ratios showed increase from 0 h to 168 h postmortem. However, the I_{2958}/I_{3303}, I_{2925}/I_{3303}, I_{2871}/I_{3303} and I_{2858}/I_{3303} ratios had the similar slight decrease at 72 h compared with 48 h and 96 h. As demonstrated in Fig. 3(a)–(e), linear regression analysis showed strong correlations between the ratios and increasing time since death. Linear regression equations of the I_{3012}/I_{3303}, I_{2958}/I_{3303}, I_{2925}/I_{3303}, I_{2871}/I_{3303}, I_{2858}/I_{3303} ratios against the PMI were shown in Table 2.

Our results show that all the ratios of C–H to N–H stretching bands increased significantly postmortem. The chemical mechanism underlying the specific changes is still unclear compared with the degradation of proteins and nucleic acids, because the chemical reactions in kidney cortex after death are so complex. However, the C–H stretching groups in 3000–2800 cm^{-1} can serve as a marker for estimating PMI due to its sequential, time-dependent process.

3.3. The absorption band region at 1700–1375 cm^{-1}

The bands at 1652 and 1541 cm^{-1} are attributed to amide I and amide II vibrations, respectively, of structural proteins [18,26,27]. The intensity of amide I remained stable, and the intensity of amide II increased postmortem. Figure 1(b) showed that there were some weak bands appearing around the band

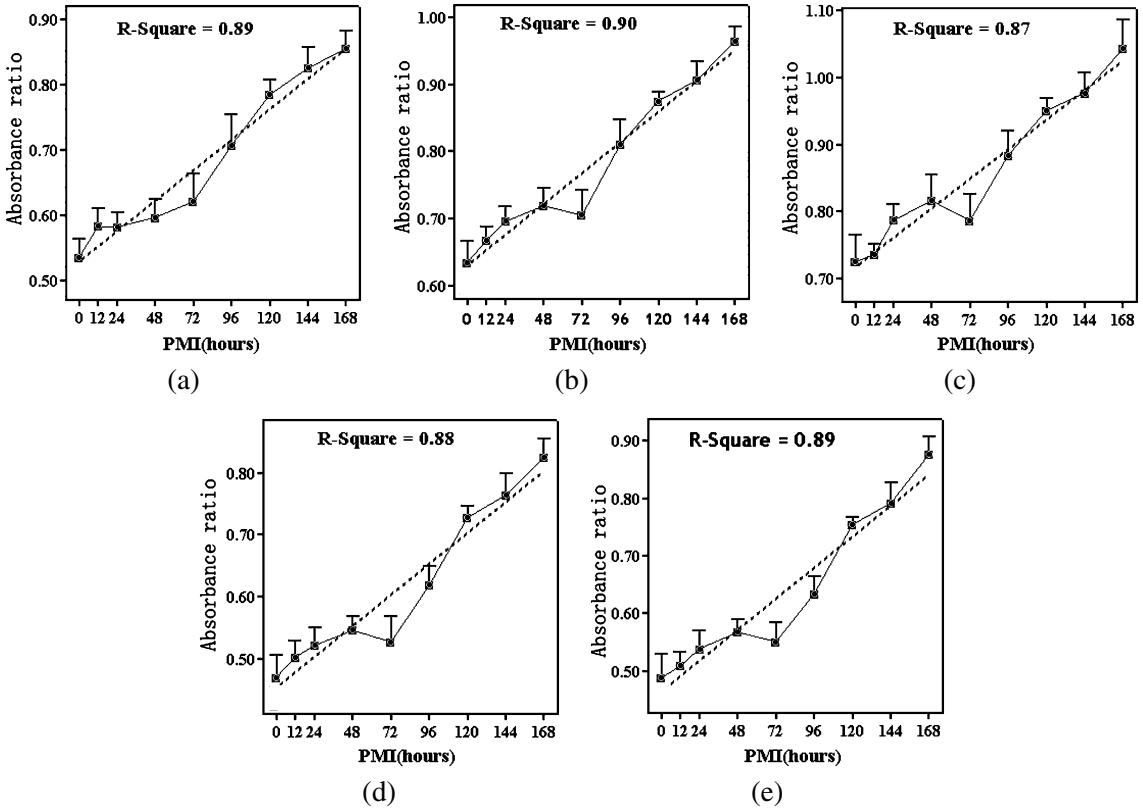

Fig. 3. Temporal FT-IR spectral intensity ratio of the bands (a) I_{3012}/I_{3303}, (b) I_{2958}/I_{3303}, (c) I_{2925}/I_{3303}, (d) I_{2871}/I_{3303}, (e) I_{2858}/I_{3303}. The fitting regression line (- - -) presented linear relationship between intensity ratio and PMI.

at 1541 cm^{-1} after 120 h postmortem in original spectra. We consider that the appearance of these weak absorption bands is closely related to increasing metabolites after death.

The band at 1456 cm^{-1}, contributed by bending vibration of the CH_2 in the lipids and proteins [25,27], slightly increased since death in the Figs 1(b) and 2. The bands at 1396 cm^{-1} is due to $CO_2{}^-$ symmetric stretching vibration of amino acid side chains and fatty acids [23,28,29]. As shown in Figs 1(b) and 2, the intensity and area of this band increase dramatically. The I_{1652}/I_{1396}, I_{1541}/I_{1396} and I_{1456}/I_{1396} ratios (Fig. 4(a)–(c)) and the A_{1652}/A_{1396}, A_{1541}/A_{1396}, A_{1456}/A_{1396} ratios (Fig. 4(d)–(f)) were used for the more precise quantitative analysis between the intensity and area ratios and the PMI. The band intensity and area ratios showed dramatic decrease with increasing time since death as shown in Fig. 4. The A_{1652}/A_{1396} ($R^2 = 0.94$) and A_{1541}/A_{1396} ratios ($R^2 = 0.95$) showed strongest linear correlations among all the ratios. As shown in Fig. 4, I_{1652}/I_{1396} ratio appeared rather variable from 12 h to 72 h postmortem.

3.4. The absorption band region at 1300–900 cm^{-1}

The bands at 1238, 1080 cm^{-1} are mainly assigned to symmetric and asymmetric stretching modes, respectively, of phosphodiester groups in nucleic acids rather than in phospholipids [22,26,27]. As shown in Figs 1(c) and 2, the intensity at 1238, 1080 cm^{-1} displayed dramatic decrease with increasing time after death. The more precise changes for 1238, 1080 cm^{-1} using the intensity bands ratios were displayed

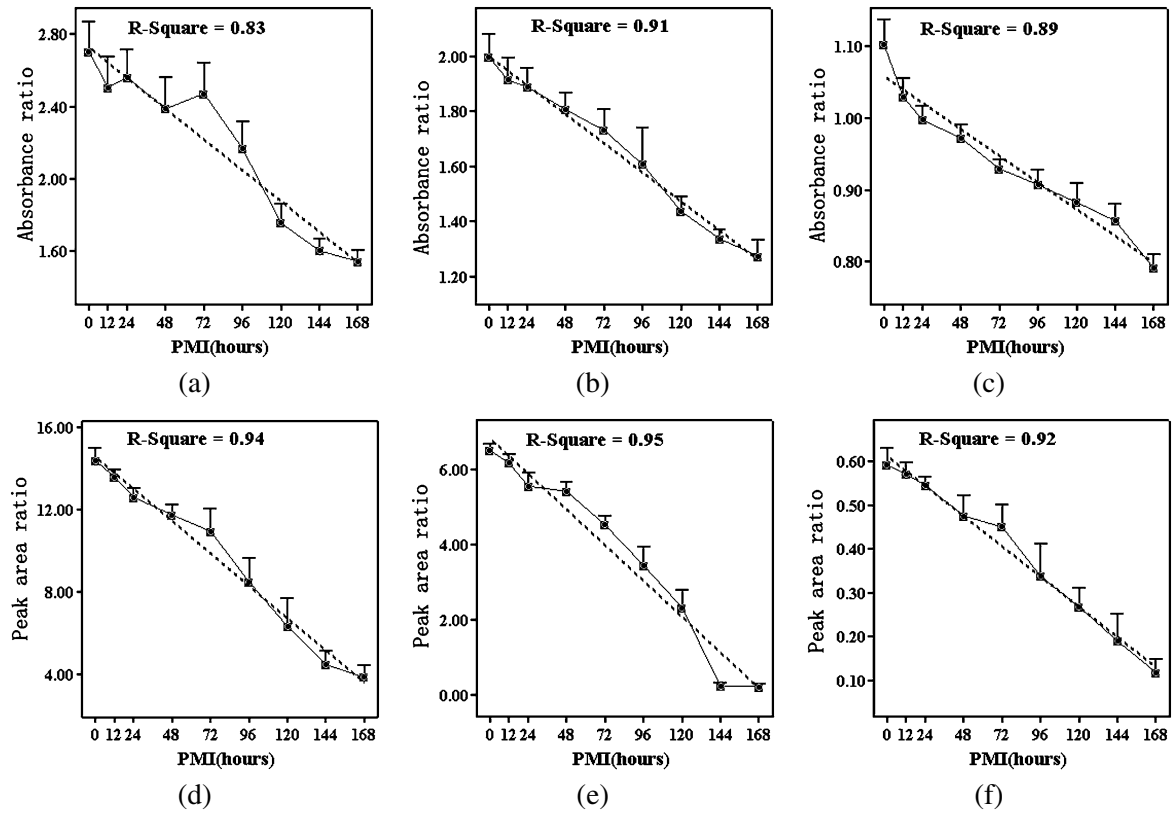

Fig. 4. Temporal FT-IR spectral intensity ratio of the bands (a) I_{1652}/I_{1396}, (b) I_{1541}/I_{1396}, (c) I_{1456}/I_{1396}. The fitting regression line (- - -) presented linear relationship between intensity ratio and PMI. Temporal FT-IR spectral area ratio of the bands (d) A_{1652}/A_{1396}, (e) A_{1541}/A_{1396}, (f) A_{1456}/A_{1396}. The fitting regression line (- - -) presented linear relationship between area ratio and PMI.

in Fig. 5. I_{1238}/I_{1396} and I_{1080}/I_{1396} ratios showed obvious decreasing linear correlations between intensity ratios and the PMI. Laura et al. [30] show that the postmortem DNA degradation occurs in porcine skeletal muscle from 3 to 56 h using single cell gel electrophoresis. However, DNA in porcine kidney cannot be detected possibly due to its autolysis. Quantification of mRNA and DNA degradation is closely correlated with the postmortem interval in autopsy cases [14–16]. Our results suggest that the FT-IR spectroscopy can be used to monitor the degradation of nucleic acid up to 168 h with high efficiency.

The bands at 1338 cm^{-1} mainly from CH_2 wagging stretching of collagen and the bands at 1170 cm^{-1} mainly from the C–O stretching modes of C–OH groups of serine, threonine, and tyrosine of proteins [18–20,25] remained the relative stable after death shown in Figs 1(c) and 2. As seen in Fig. 1(c), the band intensity at 1118 cm^{-1} remained weak and increased slightly from 0 h to 144 h after death, but the intensity presented a dramatic increase at 168 h. Some proteins, such as, calmodulin binding protein population remained relative stable for up to 96 h postmortem in rat muscle and lung. The calmodulin dependent kinase II did not change appreciably over the 96 h postmortem [13]. Therefore, the further study is needed to examine the absorption bands at 1338, 1170 and 1118 cm^{-1} as potential markers for estimating long term PMI. In addition, a new band at 1049 cm^{-1} appeared in some samples after 144 h postmortem. The

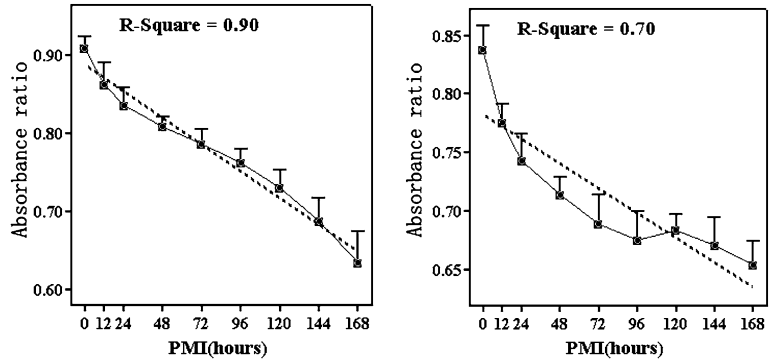

Fig. 5. Temporal FT-IR spectral intensity ratio of the bands (a) I_{1238}/I_{1396}, (b) I_{1080}/I_{1396}. The fitting regression line (- - -) presented linear relationship between intensity ratio and PMI.

Table 2
The linear regression equations of different ratios of absorption intensity and area

Numbers	Linear regression equation	x assignment	Coefficient of determination, R^2	Significance, p
1	$Y = 459.62x_1 - 235.12$	I_{3012}/I_{3303}	0.89	<0.01
2	$Y = 472.01x_2 - 289.92$	I_{2958}/I_{3303}	0.90	<0.01
3	$Y = 474.50x_3 - 330.34$	I_{2925}/I_{3303}	0.87	<0.01
4	$Y = 423.31x_4 - 182.95$	I_{2871}/I_{3303}	0.88	<0.01
5	$Y = 395.77x_5 - 175.03$	I_{2858}/I_{3303}	0.86	<0.01
6	$Y = -117.42x_6 + 333.10$	I_{1652}/I_{1396}	0.83	<0.01
7	$Y = -206.12x_7 + 419.42$	I_{1541}/I_{1396}	0.91	<0.01
8	$Y = -578.01x_8 + 619.72$	I_{1456}/I_{1396}	0.89	<0.01
9	$Y = -14.38x_9 + 214.30$	A_{1652}/A_{1396}	0.94	<0.01
10	$Y = -23.84x_{10} + 167.16$	A_{1541}/A_{1396}	0.95	<0.01
11	$Y = -320.14x_{11} + 202.17$	A_{1456}/A_{1396}	0.92	<0.01
12	$Y = -632.54x_{12} + 569.14$	I_{1238}/I_{1396}	0.90	<0.01
13	$Y = -791.61x_{13} + 642.51$	I_{1080}/I_{1396}	0.70	<0.01

Y represents postmortem interval, x represents ratio of absorption intensity and area. I: intensity of absorbance band, A: peak area of absorbance band.

appearance of this band may be considered as potential parameters for specific time point postmortem.

3.5. Analysis of other factors

There were some overlaps of ratios of absorption intensity and area at some time point postmortem as seen in Figs 3–5. However, regression analysis shows strong correlation between ratios and the PMI. Furthermore, more comprehensive analysis of different ratios will resolve the problem of overlaps. The 20($\pm$2)°C was chosen for these experiments in order to approximate a room-temperature environment. As we know, there are many factors that can influence the chemical reactions within tissues after death such as temperature [1]. Moreover, our research group has also monitored the spectral changes of rat kidney cortex at 4°C and 30°C. We found there are similar changes to the 20°C, and the spectral changes are

most dramatic at 30°C (Fig. 6). These results indicate temperature dependency of postmortem metabolic changes based on FT-IR spectra. Additionally, our research group has also used the FT-IR spectroscopy to study other rat tissues, such as lung, muscle, liver and spleen (Fig. 7), there are similar spectral changes to the kidney cortex, but the spectrum of rat kidney cortex display the most prominent changes

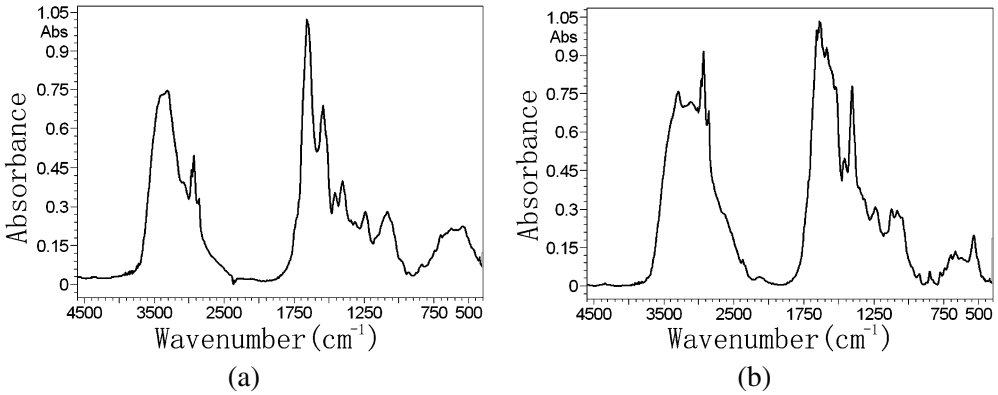

Fig. 6. FT-IR original spectra of the rat kidney cortex at 4°C (a) and 30°C (b).

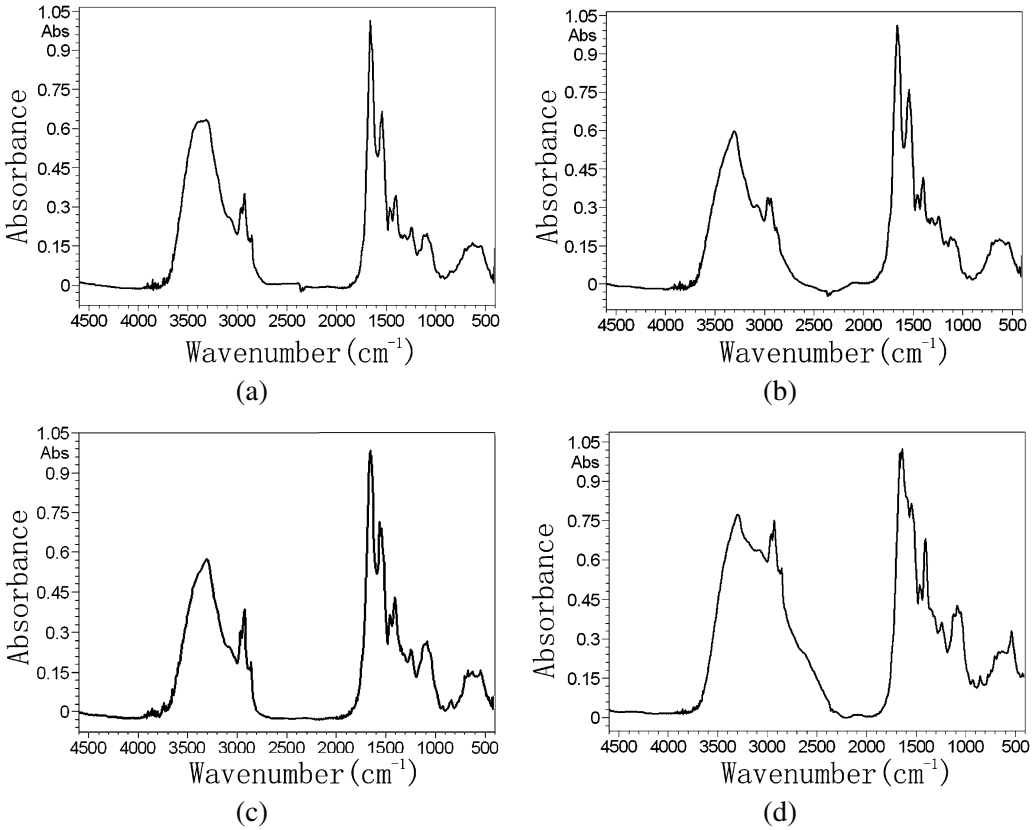

Fig. 7. FT-IR original spectra of the rat lung (a), muscle (b), liver (c) and spleen (d) at 20°C.

than the others. Further studies with human kidney cortex will be needed to verify the utility of the method.

4. Conclusion

Our results indicate that FT-IR spectroscopic analysis can monitor the postmortem metabolic changes at molecular level from 0 h to 168 h postmortem in rat kidney cortex. There were three different types of metabolic changes after death based on the spectral results: (1) increase continuously (e.g. C–H stretching region); (2) decrease continuously (e.g. PO_2^- symmetric stretching); (3) remain relatively stable (e.g. C–OH bending, CO–O–C asymmetric stretching). The absorption intensity and area ratios show close linear correlations against PMI. Additionally, FT-IR technique is a non-chemical procedure as compared with other bio-molecular methods. Therefore, it has a less influence on the chemical changes within the tissues postmortem. Besides utilizing other classical methods, FT-IR spectroscopy may be a great tool for estimating PMI at the molecular level in the forensic investigations.

Acknowledgments

The authors would like to thank Dr. Langchong He and Mr. Shaosheng Deng for their kind instruction in FT-IR spectroscopy technique. This study was funded by the Council of National Natural Science Foundation of China (No. 30471935).

References

[1] B. Knight, *Simpson's Forensic Medicine*, Oxford University Press, New York, 1996, pp. 20–28.
[2] C. Henssge and B. Madea, Estimation of the time since death, *Forensic Sci. Int.* **165** (2007), 182–184.
[3] E. Baccino, C. Cattaneo, C. Jouineau, J. Poudoulec and L. Martrille, Cooling rates of the ear and brain in pig heads submerged in water: implications for postmortem interval estimation of cadavers found in still water, *Am. J. Forensic Med. Pathol.* **28** (2007), 80–85.
[4] K. Honjyo, K. Yonemitsu and S. Tsunenari, Estimation of early postmortem intervals by a multiple regression analysis using rectal temperature and non-temperature based postmortem changes, *J. Clin. Forensic Med.* **12** (2005), 249–253.
[5] S. Banaschak, R. Rzanny, J.R. Reichenbach, W.A. Kaiser and A. Klein, Estimation of postmortem metabolic changes in porcine brain tissue using 1H-MR spectroscopy – preliminary results, *Int. J. Legal Med.* **119** (2005), 77–79.
[6] C. Henssge and B. Madea, Estimation of the time since death in the early post-mortem period, *Forensic Sci. Int.* **144** (2004), 167–175.
[7] C. Henssge, L. Althaus, J. Bolt, A. Freislederer, H.T. Haffner, C.A. Henssge, B. Hoppe and V. Schneider, Experiences with a compound method for estimating the time since death. I. Rectal temperature nomogram for time since death, *Int. J. Legal Med.* **113** (2000), 303–319.
[8] N. Lange, S. Swearer and W.Q. Sturner, Human postmortem interval estimation from vitreous potassium: an analysis of original data from six different studies, *Forensic Sci. Int.* **66** (1994), 159–174.
[9] D. Lucy, R. Aykroyd and M. Pollard, Commentary on J.I. Munoz, J.M. Suarez-Penaranda, X.L. Otero, M.S. Rodriguez-Calvo, E. Costas, X. Miguens and L. Concheiro. A new perspective in the estimation of postmortem interval (PMI) based on vitreous, *J. Forensic Sci.* **46** (2001), 1527–1528.
[10] R.A. James, P.A. Hoadley and B.G. Sampson, Determination of postmortem interval by sampling vitreous humour, *Am. J. Forensic Med. Pathol.* **18** (1997), 158–162.
[11] J.I. Munoz, J.M. Suarez-Penaranda, X.L. Otero, M.S. Rodriguez-Calvo, E. Costas, X. Miguens and L. Concheiro, A new perspective in the estimation of postmortem interval (PMI) based on vitreous, *J. Forensic Sci.* **46** (2001), 209–214.
[12] A.J. Sabucedo and K.G. Furton, Estimation of postmortem interval using the protein marker cardiac Troponin I, *Forensic Sci. Int.* **134** (2003), 11–16.

[13] S. Kang, N. Kassam, M.L. Gauthier and D.H. O'Day, Post-mortem changes in calmodulin binding proteins in muscle and lung, *Forensic Sci. Int.* **131** (2003), 140–147.
[14] S.J. Cina, Flow cytometric evaluation of DNA degradation: a predictor of postmortem interval?, *Am. J. Forensic Med. Pathol.* **15** (1994), 300–302.
[15] M. Bauer, S. Polzin and D. Patzelt, Quantification of RNA degradation by semi-quantitative duplex and competitive RT-PCR: a possible indicator of the age of bloodstains?, *Forensic Sci. Int.* **138** (2003), 94–103.
[16] M. Bauer, I. Gramlich, S. Polzin and D. Patzelt, Quantification of mRNA degradation as possible indicator of postmortem interval – a pilot study, *Leg. Med.* **5** (2003), 220–227.
[17] A. Dogan, K. Ergen, F. Budak and F. Severcan, Evaluation of disseminated candidiasis on an experimental animal model: a Fourier transform infrared study, *Appl. Spectrosc.* **61** (2007), 199–203.
[18] P.T. Wong, R.K. Wong, T.A. Caputo, T.A. Godwin and B. Rigas, Infrared spectroscopy of exfoliated human cervical cells: evidence of extensive structural changes during carcinogenesis, *Proc. Natl. Acad. Sci. USA* **88** (1991), 10988–10992.
[19] B. Rigas, S. Morgello, I.S. Goldman and P.T. Wong, Human colorectal cancers display abnormal Fourier-transform infrared spectra, *Proc. Natl. Acad. Sci. USA* **87** (1990), 8140–8144.
[20] M.A. Cohenford and B. Rigas, Cytologically normal cells from neoplastic cervical samples display extensive structural abnormalities on IR spectroscopy: implications for tumor biology, *Proc. Natl. Acad. Sci. USA* **95** (1998), 15327–15332.
[21] J. Schuttlefield, H. Al-Hosney, A. Zachariah and V.H. Grassian, Attenuated total reflection fourier transform infrared spectroscopy to investigate water uptake and phase transitions in atmospherically relevant particles, *Appl. Spectrosc.* **61** (2007), 283–292.
[22] G. Cakmak, I. Togan and F. Severcan, 17Beta-estradiol induced compositional, structural and functional changes in rainbow trout liver, revealed by FT-IR spectroscopy: a comparative study with nonylphenol, *Aquat. Toxicol.* **77** (2006), 53–63.
[23] F. Severcan, N. Kaptan and B. Turan, Fourier transform infrared spectroscopic studies of diabetic rat hear crude membranes, *Spectrosc. – Int. J.* **17** (2003), 569–577.
[24] C.J. Thompson, R.G. Riley, J.E. Amonette and P.L. Gassman, Quantification of volatile organics in soil aging experiments using fourier transform infrared spectroscopy, *Appl. Spectrosc.* **60** (2006), 914–919.
[25] G. Cakmak, I. Togan, C. Uguz and F. Severcan, FT-IR spectroscopic analysis of rainbow trout liver exposed to nonylphenol, *Appl. Spectrosc.* **57** (2003), 835–841.
[26] B. Stuart, *Infrared Spectroscopy: Fundamentals and Applications*, John Wiley & Sons Ltd., West Sussex, 2004, pp. 137–163.
[27] S. Gaudenzi, D. Pozzi, P. Toro, I. Silvestri, S. Morrone and A.C. Castellano, Cell apoptosis specific marker found by Fourier Transform Infrared Spectroscopy, *Spectrosc. – Int. J.* **17** (2004), 569–577.
[28] N. Toyran, P. Lasch, D. Naumann, B. Turan and F. Severcan, Early alterations in myocardia and vessels of the diabetic rat heart: an FTIR microspectroscopic study, *Biochem. J.* **397** (2006), 427–436.
[29] F. Severcan, G. Gorgulu, S.T. Gorgulu and T. Guray, Rapid monitoring of diabetes-induced lipid peroxidation by Fourier transform infrared spectroscopy: evidence from rat liver microsomal membranes, *Anal. Biochem.* **339** (2005), 36–40.
[30] L.A. Johnson and J.A. Ferris, Analysis of postmortem DNA degradation by single-cell gel electrophoresis, *Forensic Sci. Int.* **126** (2002), 43–47.